

ULB–TH 99/19
October 1999

Neutrino gravitational lensing

R. Escribano¹, J.-M. Frère², D. Monderen and V. Van Elewyck

*Service de Physique Théorique, Université Libre de Bruxelles, CP 228, B-1050 Bruxelles,
Belgium*

Abstract

We study the lensing of neutrinos by astrophysical objects. At the difference of photons, neutrinos can cross a stellar core; as a result the lens quality improves. While Uranians alone would benefit from this effect in the Sun, similar effects could be considered for binary systems.

¹Chercheur I. I. S. N.

²Directeur de recherches du F. N. R. S.

1 Introduction

In this note we want to investigate the possibility of neutrino lensing by astrophysical objects (stars, galaxies or rather galactic halo). At the difference of photons, neutrinos can cross even a star's core. As will be seen below this results in a much better focalisation. On the other hand, the price to pay is the extreme difficulty to detect neutrinos, and the comparatively poor angular resolution of "neutrino telescopes". For this reason, the only thing we can hope for is a signal intensification, rather than the spectacular photon lensing patterns. The main equations are established in section 2, with details in the Appendix. Section 3 deals with neutrino interactions in a stellar medium, and specify which energy range can be studied in this way. In section 4 we consider a number of situations and establish the corresponding signal enhancement expected. Finally in section 5 we consider some practical examples. It appears clearly that the Earth - Sun distance is too small for a sizable effect to take place, (an observatory on Uranus would notice the enhancement of distant neutrino sources whenever they are aligned with the Sun). We then consider the case of galaxies, through their halo. We finally turn to binary systems. We will not in this paper comment on the possible origin of energetic neutrinos, but we remark that an interesting situation is met when one of the companions focuses the neutrino flux originating from the other.

2 Gravitational deflection of neutrinos

In this section we study the deflection of neutrinos from straight-line motion as they pass through a gravitational field produced by a compact object of mass M . We will distinguish two cases: when the neutrino flux passes far away from the object (OUTside solution), a situation equivalent to the gravitational lensing of photons, and, when the neutrino flux passes through the object (INside solution). In the latter case, we consider three specific cases depending on the compact object density profile: constant density (an academic but constructive example), Gaussian distribution density (suitable for stars³), and Lorentzian distribution density (which could be associated

³ The density profile of stars is not exactly Gaussian but we use it here in order to obtain simple analytical results. Such a description should be considered as a good approximation

to a galactic halo⁴).

We begin by calculating the trajectory of a massless neutrino (or with mass very small compared to its energy) in the Schwartzschild metric under the assumption that M/r is everywhere small along the trajectory [1]. The equation of the orbit is⁵

$$\frac{d\phi}{dr} = \frac{1}{r^2 \sqrt{\frac{1}{b^2} - \frac{1}{r^2} \left(1 - \frac{2M}{r}\right)}}, \quad (1)$$

where b is defined as the impact parameter. Using the definition $u \equiv \frac{1}{r}$:

$$\frac{d\phi}{du} = \frac{1}{\sqrt{\frac{1}{b^2} - u^2 + 2Mu^3}}. \quad (2)$$

If we neglect the u^3 term in Eq. (2), all effects of M disappear, and the solution is

$$r \sin(\phi - \phi_0) = b, \quad (3)$$

a straight line. In the limit $Mu \ll 1$, or $R_{\text{Sch.}} \equiv 2M \ll b$, if we define $y \equiv u(1 - Mu)$, Eq. (2) becomes

$$\frac{d\phi}{dy} = \frac{1 + 2My}{\sqrt{\frac{1}{b^2} - y^2}} + O(M^2 u^2). \quad (4)$$

Integrating Eq. (4) gives

$$\phi_{\text{OUT}}(y) = \phi_0 + \frac{2M}{b} + \arcsin(by) - 2M \sqrt{\frac{1}{b^2} - y^2}, \quad (5)$$

where the integration constant is defined as $\phi = \phi_0$ (with ϕ_0 the incoming direction) when the initial trajectory has $r \rightarrow \infty$ (or $y \rightarrow 0$). The particle reaches its smallest r when $\frac{dr}{d\lambda} = 0$:

$$\frac{dr}{d\lambda} = E \sqrt{1 - \left(1 - \frac{2M}{r}\right) \frac{b^2}{r^2}} = 0 \implies y_{\text{max}} = \frac{1}{b} + O(M^2 u^2). \quad (6)$$

to the real case.

⁴ The Lorentzian profile behaves as $1/r^2$ for large r , in agreement with velocity dispersion curves for galaxies and clusters.

⁵Geometrized units $c = G = 1$ are used throughout the paper.

This occurs at the angle

$$\phi_{\text{OUT}}(y = \frac{1}{b}) = \phi_0 + \frac{2M}{b} + \frac{\pi}{2} . \quad (7)$$

It has thus passed through an angle $\frac{2M}{b} + \frac{\pi}{2}$ as it travels to its point of closest approach. By symmetry, it passes through a further angle of the same size as it moves outwards from its point of closest approach (see Ref. [1]). Then, the particle passed through a total angle of $\frac{4M}{b} + \pi$. If it were keeping to a straight trajectory, this angle would be π , so the net deflection is

$$\Delta\phi_{\text{OUT}} = \frac{4M}{b} . \quad (8)$$

For the case of a neutrino flux passing through the object, we must first, in order to study the neutrino trajectory, look for the form of the space-time in the region inside the object. Here, we restrict ourselves to the case of static spherically symmetric space-times⁶. In that case, the most general metric is (see Ref. [1] for details):

$$ds^2 = -e^{2\Phi(r)} dt^2 + e^{2\Lambda(r)} dr^2 + r^2 d\Omega^2 , \quad (9)$$

where it is convenient to replace $\Lambda(r)$ by

$$m(r) \equiv \frac{1}{2}r \left(1 - e^{-2\Lambda}\right) \implies g_{rr} = e^{2\Lambda} = \frac{1}{1 - \frac{2m(r)}{r}} . \quad (10)$$

For a static perfect fluid⁷, Einstein equations imply

$$\begin{aligned} \frac{dm(r)}{dr} &= 4\pi r^2 \rho(r) , \\ \frac{d\Phi(r)}{dr} &= \frac{m(r) + 4\pi r^3 p(r)}{r(r - 2m(r))} = -\frac{1}{\rho(r) + p(r)} \frac{dp(r)}{dr} , \end{aligned} \quad (11)$$

⁶Spherically symmetric space-times are reasonably simple, yet physically very important, since very many objects of importance in astrophysics appear to be nearly spherical. A static space-time is defined to be one in which we can find a time coordinate t with two properties: (i) all metric components are independent of t , and (ii) the geometry is unchanged by time reversal, $t \rightarrow -t$.

⁷A perfect fluid in relativity is defined as a fluid that has no viscosity and no heat conduction in the momentarily comoving reference frame (MCRF). A static fluid is a fluid that has no motion.

where $\rho(r)$, $m(r)$ and $p(r)$ are, respectively, the density, mass and pressure of the object at a radius r . For completeness, in the region outside the object we have $p = \rho = 0$, then

$$\begin{aligned} m(r) = M = \text{const.} &\implies e^{2\Phi(r)} = 1 - \frac{2M}{r} \\ \implies ds^2 &= -\left(1 - \frac{2M}{r}\right) dt^2 + \frac{dr^2}{1 - \frac{2M}{r}} + r^2 d\Omega^2. \end{aligned} \quad (12)$$

In the region inside the object, exact solutions to the relativistic equations are very hard to solve analytically for a given equation of state [1]. One interesting exact solution is the Schwarzschild constant-density interior solution, which we use here as an example of the framework needed to study other density profiles.

Inside R , where R is the physical radius of the object, $\rho \neq 0, p \neq 0$. For a constant density profile $\rho(r) = \rho$, the equation of the orbit is (see the appendix for a detailed calculation)

$$\frac{d\phi}{dr} = \frac{\frac{3}{2}\sqrt{1 - \frac{2M}{R}} - \frac{1}{2}\sqrt{1 - \frac{2M}{R}\frac{r^2}{R^2}}}{\sqrt{1 - \frac{2M}{r}\left(\frac{r}{R}\right)^3}} \frac{1}{r^2 \sqrt{\frac{1}{b^2} - \frac{1}{r^2} \left(\frac{3}{2}\sqrt{1 - \frac{2M}{R}} - \frac{1}{2}\sqrt{1 - \frac{2M}{R}\frac{r^2}{R^2}}\right)^2}}, \quad (13)$$

and the net deflection is

$$\Delta\phi = \begin{cases} \frac{4M}{b} & \text{if } b \geq R \\ \frac{4M}{b} \left(1 - \sqrt{1 - \frac{b^2}{R^2}}\right) + 2 \arcsin \left[\frac{b}{R} \left(1 - \frac{M}{R}\right)\right] \\ \quad + \frac{3M}{R} \frac{b}{R} \sqrt{1 - \frac{b^2}{R^2}} - 2 \arcsin \left\{\frac{b}{R} \left[1 - \frac{3M}{2R} \left(1 - \frac{b^2}{3R^2}\right)\right]\right\} & \text{if } b < R \end{cases} \quad (14)$$

where the outside solution is also included for completeness.

Next, we analyze the solutions for the Gaussian and Lorentzian distribution densities. The Gaussian profile is a convenient approximation to the mass distribution in stars, while the Lorentzian profile is valid for galactic halos. In both cases, it is possible to neglect the pressure with respect to the mass density, $p \ll \rho$ (see Ref. [1] for the so-called Newtonian stars), so we also have $4\pi r^3 p \ll m$. Moreover, the metric must be nearly flat, so in Eq. (10) we require $m(r) \ll r$. These inequalities simplify Eq. (11) to

$$\frac{d\Phi(r)}{dr} = \frac{m(r)}{r^2}, \quad (15)$$

and the metric in Eq. (9) to

$$e^{2\Lambda(r)} \simeq 1 + \frac{2m(r)}{r} \quad \text{and} \quad e^{2\Phi(r)} \simeq 1 + 2\Phi(r) \quad (16)$$

$$\implies ds^2 = -(1 + 2\Phi(r))dt^2 + \left(1 + \frac{2m(r)}{r}\right)dr^2 + r^2d\Omega^2 .$$

For the case of a Gaussian density profile $\rho(r) = \rho_0 e^{-r^2/r_0^2}$, the equation of the orbit is (see appendix for details)

$$\begin{aligned} \frac{d\phi}{dr} = & \left[1 - \frac{M}{R} \frac{e^{(R^2-r^2)/r_0^2}-1}{r_0/R e^{R^2/r_0^2} \sqrt{\pi}/2 \operatorname{erf}(R/r_0)-1} \right] \\ & \times \frac{1}{r^2 \sqrt{\frac{1}{b^2} - \frac{1}{r^2} \left[1 - \frac{2M}{R} \frac{r_0/r e^{R^2/r_0^2} \sqrt{\pi}/2 \operatorname{erf}(r/r_0)-1}{r_0/R e^{R^2/r_0^2} \sqrt{\pi}/2 \operatorname{erf}(R/r_0)-1} \right]} } , \end{aligned} \quad (17)$$

where the error function is defined as $\operatorname{erf}(z) = \frac{2}{\sqrt{\pi}} \int_0^z dt e^{-t^2}$. The net deflection is then

$$\Delta\phi = \begin{cases} \frac{4M}{b} & \text{if } b \geq R \\ \frac{4M}{b} \left(1 - \sqrt{1 - \frac{b^2}{R^2}} \right) + \frac{4M}{b} \frac{r_0/R e^{R^2/r_0^2} \sqrt{\pi}/2}{r_0/R e^{R^2/r_0^2} \sqrt{\pi}/2 \operatorname{erf}(R/r_0)-1} \\ \quad \times \left[\sqrt{1 - \frac{b^2}{R^2}} \operatorname{erf}(R/r_0) - e^{-b^2/r_0^2} \operatorname{erf}\left(\sqrt{1 - \frac{b^2}{R^2}} \frac{R}{r_0}\right) \right] & \text{if } b < R \end{cases} \quad (18)$$

It is very interesting (because we are close to a real case) to compare the previous result with a naïve approximation where for a given impact parameter b one studies the net deflection by a sphere of radius b and identical density profile

$$\begin{aligned} \Delta\phi|_{\text{approx}} &\equiv \frac{4m(b)}{b} \\ &= \frac{4M}{R} e^{(R^2-r^2)/r_0^2} \frac{r_0/r e^{r^2/r_0^2} \sqrt{\pi}/2 \operatorname{erf}(r/r_0)-1}{r_0/R e^{R^2/r_0^2} \sqrt{\pi}/2 \operatorname{erf}(R/r_0)-1} \quad \text{for } b < R \end{aligned} \quad (19)$$

In Fig. 1, we plot for comparison the exact result in Eq. (18) together with the naïve approximation in Eq. (19). We have taken the Sun as example of a typical star. Then, the mass and the radius in Eqs. (18,19) are fixed to $M \equiv M_\odot = 1.48 \text{ km}$ and $R \equiv R_\odot = 6.96 \times 10^5 \text{ km}$. The parameter r_0 is taken to be $r_0 = 0.2R_\odot$. As it is seen from Fig. 1, the maximal net deflection

occurs at $b \simeq r_0$ and is $\Delta\phi(b \simeq r_0) \simeq 3.2\Delta\phi(b = R_\odot)$, showing that the lensing effect inside the star is bigger than the outside effect (except for $b \leq 0.04R_\odot$). It is also shown that for the naïve approximation the maximal deflection is displaced up to $b \simeq 1.5r_0$ and its value is around 20% smaller than for the exact result. So then, our calculation seems to be essential for a detailed analysis of the gravitational lensing of a neutrino beam by a star.

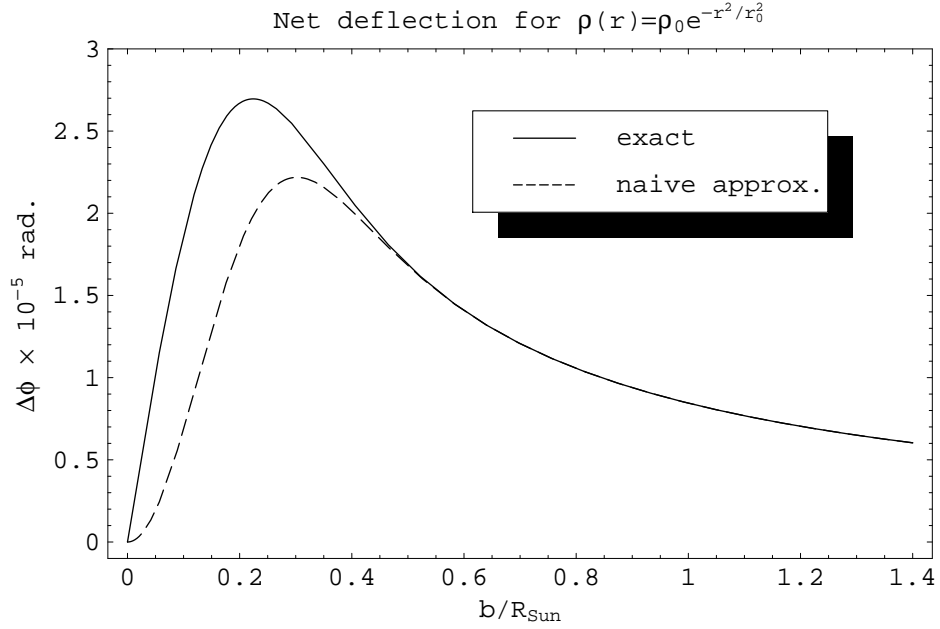


Figure 1: Net deflection $\Delta\phi$ as a function of the impact parameter b for the case of a Gaussian density profile $\rho(r) = \rho_0 e^{-r^2/r_0^2}$ (see Eq. (18)). The naïve approximation of Eq. (19) is also included for comparison. In both curves, $M \equiv M_\odot = 1.48$ km, $R \equiv R_\odot = 6.96 \times 10^5$ km and $r_0 = 0.2R_\odot$ are used.

For the case of a Lorentzian density profile $\rho(r) = \frac{\rho_0}{1+r^2/r_0^2}$, the equation

of the orbit is

$$\frac{d\phi}{dr} = \frac{\left[1 + \frac{M}{R} \frac{\frac{1}{2} \log\left(\frac{r^2+r_0^2}{R^2+r_0^2}\right)}{1-r_0/R \arctan(R/r_0)} \right]}{r^2 \sqrt{\frac{1}{b^2} - \frac{1}{r^2} \left[1 - \frac{2M}{R} \frac{1-r_0/r \arctan(r/r_0) - \frac{1}{2} \log\left(\frac{r^2+r_0^2}{R^2+r_0^2}\right)}{1-r_0/R \arctan(R/r_0)} \right]}}, \quad (20)$$

and the final deflection is

$$\Delta\phi = \begin{cases} \frac{4M}{b} & \text{if } b \geq R \\ \frac{4M}{b} \left(1 - \sqrt{1 - \frac{b^2}{R^2}} \right) - \frac{4M}{b} \frac{1}{1-r_0/R \arctan(R/r_0)} \frac{r_0}{R} \\ \times \left[\begin{aligned} &\sqrt{1 - \frac{b^2}{R^2}} \arctan(R/r_0) \\ & - \sqrt{1 + \frac{b^2}{r_0^2}} \arctan\left(\frac{\sqrt{1 - \frac{b^2}{R^2}} R}{\sqrt{1 + \frac{b^2}{r_0^2}} r_0} \right) \end{aligned} \right] & \text{if } b < R \end{cases} \quad (21)$$

Here, it is also interesting to compare the previous result with the naïve approximation for a Lorentzian density profile

$$\Delta\phi|_{\text{approx}} = \frac{4M}{R} \frac{1 - r_0/r \arctan(r/r_0)}{1 - r_0/R \arctan(R/r_0)} \quad \text{for } b < R \quad (22)$$

In Fig. 2, we plot the exact result in Eq. (21) and the naïve approximation in Eq. (22). Here, we have taken $M \equiv M_{\text{Galaxy}} = 10^{12} M_{\odot}$ and $R \equiv R_{\text{Galaxy}} = 100$ kpc as an example for galaxies. In this case, with $r_0 = 0.2 R_{\text{Galaxy}}$, the maximal net deflection occurs at $b \simeq 3r_0$ and is around 15% bigger than the value at $b = R_{\text{Galaxy}}$, while for the naïve approximation the lensing effect inside the galactic halo is always smaller than the effect at $b = R_{\text{Galaxy}}$. Again, we think that a detailed calculation is convenient.

As a summary of this section, we plot in Fig. 3 the normalized net deflection $\Delta\phi/\Delta\phi(b=R)$ as a function of the normalized impact parameter b/R for the three specific density profiles considered along the analysis: constant density, Gaussian and Lorentzian distribution densities. Such a normalization allows for a clear comparison among the three profiles and is independent

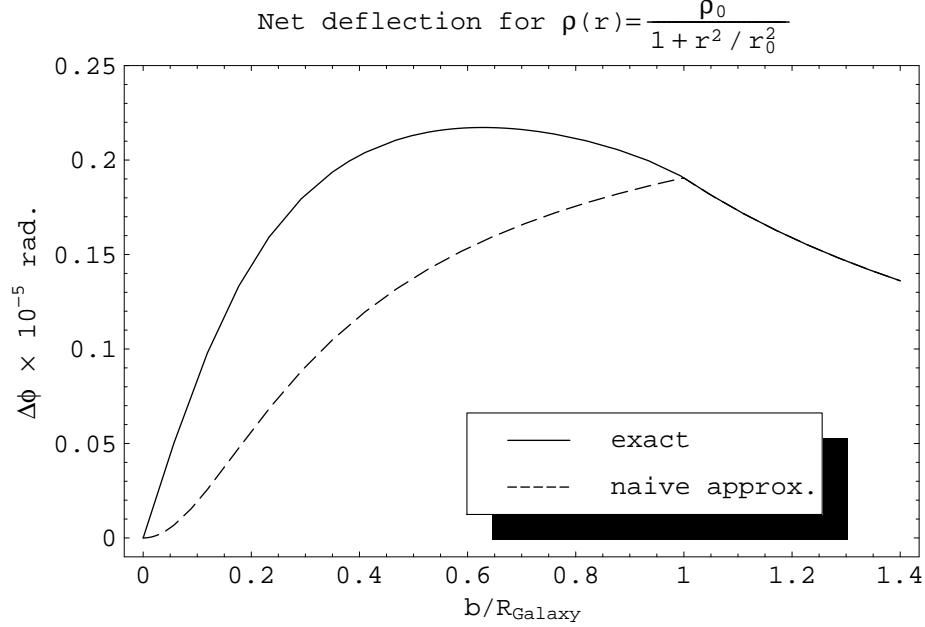


Figure 2: The same as in Fig. 1 but for a Lorentzian density profile $\rho(r) = \frac{\rho_0}{1+r^2/r_0^2}$. $M \equiv M_{\text{Galaxy}} = 10^{12} M_{\odot}$, $R \equiv R_{\text{Galaxy}} = 100$ kpc and $r_0 = 0.2 R_{\text{Galaxy}}$ are used.

of the mass and physical radius of the compact object. Only for the case of stars (Gaussian profile) the lensing effect at the interior of the star is substantially amplified with respect to the outside effect (the inside effect should be compared with the effect at $b = R$). For galactic halos, the maximal inside net deflection is slightly bigger than at $b = R$, while for an object of constant density the inside lensing effect is always smaller than at $b = R$.

Finally, we plot the focal length f as a function of the impact parameter b . The focal length is defined as the distance at which the lens focuses the signal (see Sec. 4 for details)

$$\Delta\phi = \frac{b}{f(b)} . \quad (23)$$

In Fig. 4, the (normalized) focal lengths for the three different profiles are

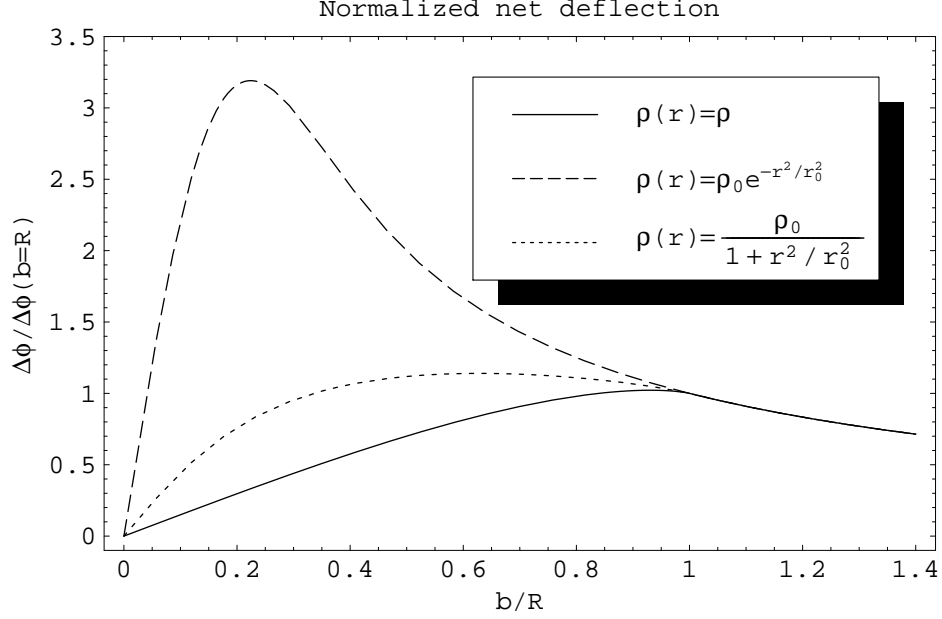


Figure 3: Normalized net deflection $\Delta\phi/\Delta\phi(b = R)$ as a function of the normalized impact parameter b/R for a constant density profile (solid line), a Gaussian density profile (dashed line) and a Lorentzian density profile (dotted line). In the last two cases, r_0 is taken to be $r_0 = 0.2R$.

drawn. At $b \ll R$

$$\frac{f(b \ll R)}{f(b = R)} = \begin{cases} \frac{2}{3} & \text{for } \rho(r) = \rho \\ \frac{r_0/R e^{R^2/r_0^2} \sqrt{\pi}/2 \operatorname{erf}(R/r_0) - 1}{e^{R^2/r_0^2} \sqrt{\pi}/2 \operatorname{erf}(R/r_0)} \frac{r_0}{R} & \text{for } \rho(r) = \rho_0 e^{-r^2/r_0^2} \\ 2 \frac{1 - r_0/R \arctan(R/r_0)}{\arctan(R/r_0)} \frac{r_0}{R} & \text{for } \rho(r) = \frac{\rho_0}{1 + r^2/r_0^2} \end{cases} \quad (24)$$

We postpone to Sec. 4 (where focal lengths are discussed in detail) the comments about the quality of the different gravitational lenses considered here.

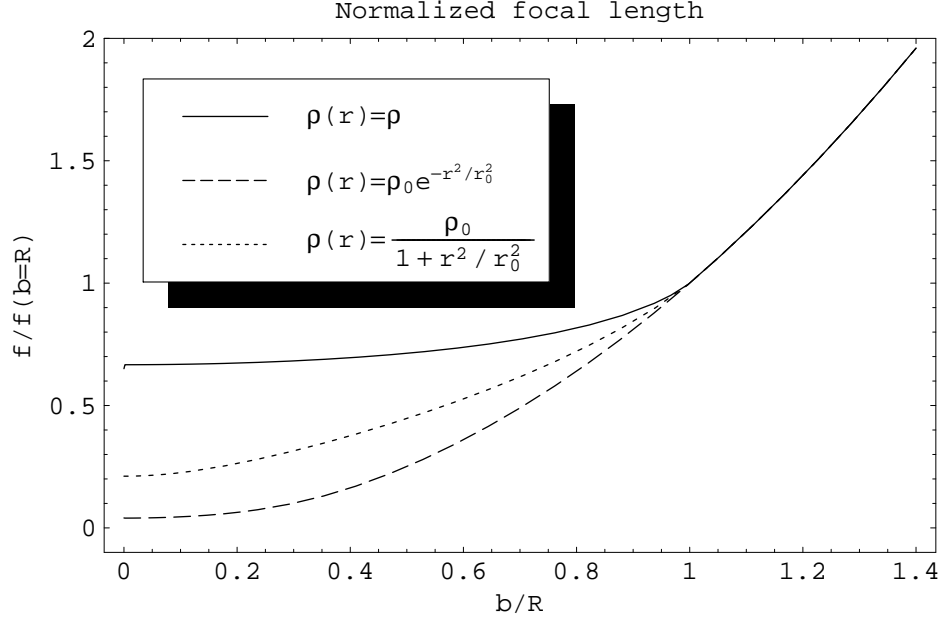


Figure 4: Normalized focal length $f/f(b = R)$ as a function of the normalized impact parameter b/R .

3 Neutrino absorption

While neutrinos are able to travel *across* the massive object, we have to consider their interactions with the matter inside; these will indeed reduce the neutrino flux and thus the efficiency of the signal amplification gained through lensing. At the energies of interest for cosmic neutrinos ($E \geq 1 - 10 \text{ GeV}$), we have deep inelastic scattering off individual nucleons. Charged currents will cause the conversion of neutrinos into charged leptons, which will later be absorbed or decay, while neutral interactions will deflect them by angles in general large compared to the lensing effect. In both cases, the interacting neutrinos will be lost for lensing amplification.

Calling σ the interaction cross-section (which depends on the neutrino energy) and $N(x)$ the number density of scatterers along the neutrino path, we have the well-known formula for an infinitesimal flux variation due to

interaction with matter:

$$d\Phi = N(x) \cdot \sigma(E_\nu) \cdot \Phi \cdot dx \quad (25)$$

The neutrino flux attenuation after passing through a layer of matter of depth x is thus given by:

$$\Phi(x, E_\nu) = \Phi_0 e^{-\sigma(E_\nu) \int_0^x N(x') dx'} \quad (26)$$

Here we deal with objects having a spherical symmetry, so it is easier to express Eq. (26) in terms of the radial variable $r = \sqrt{x^2 + b^2}$, b being the impact parameter of the neutrino respect to the center of the object. We then get

$$\Phi(b, E_\nu) = \Phi_0 e^{-2\sigma(E_\nu) \int_b^R N(r) \frac{r dr}{\sqrt{r^2 - b^2}}} \quad (27)$$

where R is the radius of the object. To solve this equation, we need to collect information on the relevant cross-sections, the possible mass density profiles and the composition of the object (that is, how to relate mass density to number density).

3.1 Neutrino cross-sections

At current accelerator energies, neutrino-proton and neutrino-neutron scattering differ (as the valence quark content is different), as do neutrino and antineutrino interactions. From experimental results [3, 4], we adopt the following approximations :

$$\begin{aligned} \sigma_{tot}^{\nu p} &= 0.89 \sigma_{CC}^{\nu N} & \sigma_{tot}^{\bar{\nu} p} &= 1.70 \sigma_{CC}^{\bar{\nu} N} \\ \sigma_{tot}^{\nu n} &= 1.70 \sigma_{CC}^{\nu N} & \sigma_{tot}^{\bar{\nu} n} &= 1.03 \sigma_{CC}^{\bar{\nu} N} \end{aligned} \quad (28)$$

using the tables of values for neutrino-isoscalar nucleon from Quigg, Reno *et al.* [2]

Above 10^6 GeV all these interactions become identical as sea quarks largely dominate. We may thus directly use the values for scattering on an isoscalar nucleon (again from [2]) :

$$\sigma_{tot}^{(\bar{\nu})p} = \sigma_{tot}^{(\bar{\nu})n} = \sigma_{tot}^{(\bar{\nu})N} \quad (29)$$

Strictly speaking we should interpolate between those two situations using appropriate structure functions, however, in view of the results, the above approximations are sufficient.

Due to the smallness of the ratio $\frac{m_e}{m_{nucleon}}$, neutrino-electron interactions will be neglected compared to neutrino-nucleon ones, except in the particular case of the Glashow resonance $\bar{\nu}_e e^- \rightarrow W^- \rightarrow anything$, that occurs at an energy $E_{\bar{\nu}_e} = 6.3$ PeV. At that energy we have [5]

$$\sigma^{\bar{\nu}_e e^-} \simeq 5 \times 10^{-31} \text{ cm}^2 \quad (30)$$

Having taken into account the various components of the cross section, we rewrite the formula (27) giving the transmission probability of the neutrino as:

$$P_T(b, E_\nu) = \exp \left[-2 \sum_X \sigma^{\nu X}(E_\nu) \int_b^R N_X(r) \frac{r dr}{\sqrt{r^2 - b^2}} \right] \quad (31)$$

where X stands for each kind of scatterer. The number densities $N_X(r)$ depend on the composition and mass density profile of the lens in the following obvious way :

$$N_X(r) = \frac{\mathcal{M}_X}{M_X} \rho(r) \quad (32)$$

where \mathcal{M}_X and M_X are respectively the fraction in mass and the molar mass of constituent X; ρ is the mass density of the lens. Let us now investigate the probability of transmission for the two particular cases of physical relevance that have been discussed in the previous section, i.e. stars and galaxies :

3.2 Neutrino transmission through a star

All the following calculations apply in a good approximation to all the Sun-like stars ⁸. We will suppose that the star is made up of 25 % of Helium and 75 % of Hydrogen in number; we then get the following relations between number and mass densities :

$$N_{He}(r) = 0.142 \text{ mol } \left(\frac{\rho(r)}{1 \text{ gr}} \right) \quad (33)$$

$$N_H(r) = 0.427 \text{ mol } \left(\frac{\rho(r)}{1 \text{ gr}} \right) \quad (34)$$

⁸Neutrino flux attenuation in the Sun has also been considered in [6].

that we used in our numerical calculations. We adopted for the mass density profile a Gaussian distribution (normalized to the total mass M , in the approximation $r_0 < 0.4R$) that reads:

$$\rho(r) = \frac{1}{\pi^{3/2} \text{erf}(\frac{R}{r_0})} \frac{M}{r_0^3} e^{-(\frac{r}{r_0})^2} \quad (35)$$

in function of the total mass M and radius R of the star, for a distribution in which most of the object's mass is concentrated in a sphere of radius r_0 (we have normalized to the total mass). We performed detailed calculations in the case $r_0 = \frac{R}{5}$; using Eqs. (32) and (35) the transmission probability $P_T = \frac{\Phi}{\Phi_0}$ (31) then becomes

$$\begin{aligned} P_T(b, E_\nu) &= \exp \left\{ -\frac{250}{\pi^{3/2} \text{erf}(5)} \frac{M}{R^3} \left[\sigma^{\nu_{He}} \frac{\mathcal{M}_{He}}{M_{He}} + \sigma^{\nu_H} \frac{\mathcal{M}_H}{M_H} \right] \times \right. \\ &\quad \times \left. \int_b^R e^{-(\frac{5r}{R})^2} \frac{r dr}{\sqrt{r^2 - b^2}} \right\} \\ &= \exp \left\{ -\frac{25}{\pi} \frac{M}{R^2} \frac{\text{erf}(5\sqrt{1 - \frac{b^2}{R^2}})}{\text{erf}(5)} e^{-(\frac{5b}{R})^2} \times \right. \\ &\quad \times \left. \left[\sigma^{\nu_p} \left(2\frac{\mathcal{M}_{He}}{M_{He}} + \frac{\mathcal{M}_H}{M_H} \right) + \sigma^{\nu_n} \left(2\frac{\mathcal{M}_{He}}{M_{He}} \right) \right] \right\} \end{aligned} \quad (36)$$

We present in Fig. 5 and 6 the plots of the transmission probability of neutrinos across the Sun as a function of b/R_\odot ; we have added the density profile on the same figure. For antineutrinos we have drawn the curve at $E_{\bar{\nu}_e} = 6.3$ PeV where $\bar{\nu}_e e^-$ is dominant; in this particular case, transmission probability can be written as

$$\begin{aligned} P_T(b, 6.3 \text{PeV}) &= \exp \left\{ -\frac{25}{\pi} \frac{M}{R^2} \frac{\text{erf}(5\sqrt{1 - \frac{b^2}{R^2}})}{\text{erf}(5)} e^{-(\frac{5b}{R})^2} \times \right. \\ &\quad \times \left. \sigma^{\bar{\nu}_e e^-}(6.3 \text{PeV}) \left[2\frac{\mathcal{M}_{He}}{M_{He}} + \frac{\mathcal{M}_H}{M_H} \right] \right\} \end{aligned} \quad (37)$$

as electron and proton densities are supposed to be equal in stars.

As we see from Fig. 5 and 6, neutrinos with energies of 1 TeV or more are completely absorbed or scattered away in the core of the star. Even at 100

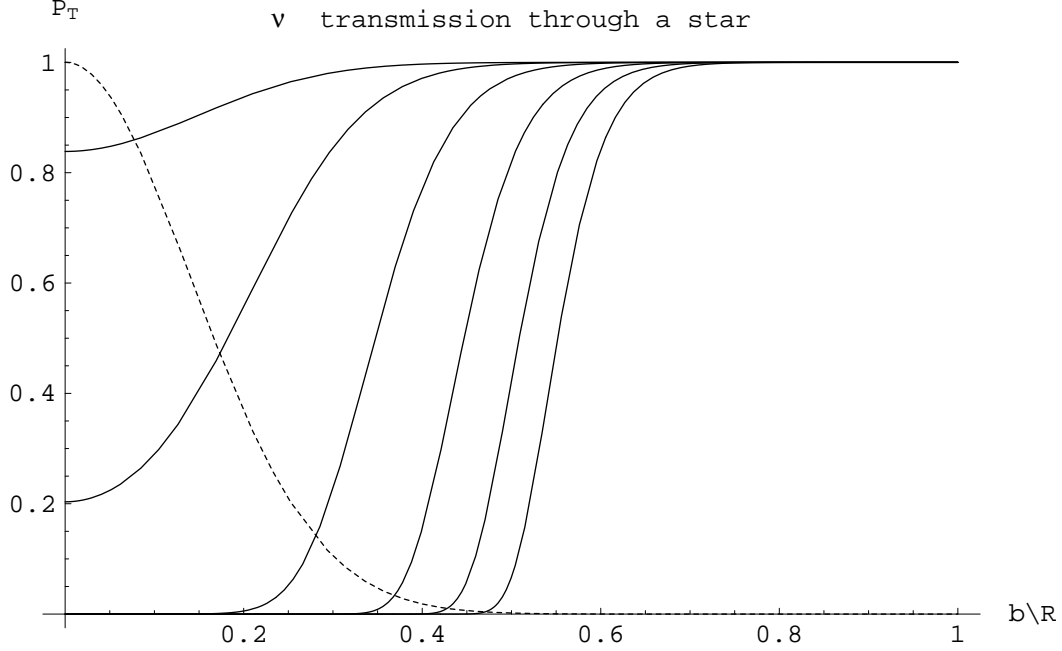


Figure 5: Transmission probability in function of b , the impact parameter, for a neutrino energy $E_\nu = 10$ GeV, 10^2 GeV, 10^3 GeV, 10^4 GeV, 10^5 GeV, 10^6 GeV (solid lines, from left to right); the Gaussian density profile $\rho(r) = e^{-(\frac{5r}{R})^2}$ is the dotted line.

GeV the interactions are frequent enough to significantly attenuate the flux of neutrinos coming out of the star. Unfortunately, the zone where lensing could be the most efficient (as the star's core acts as a "real lens") is thus ruled out because of flux attenuation for neutrinos of energy 100 GeV or more. But we can see that under 100 GeV, interactions of neutrinos inside the star have nearly no incidence on the outcoming flux, which is totally recovered after lensing by the star.

3.3 Neutrino transmission through a galaxy

Neutrinos passing through a galaxy may interact either with its visible matter or with the surrounding halo of massive relic neutrinos. These last interactions become significant only for incoming neutrinos at ultra high energies

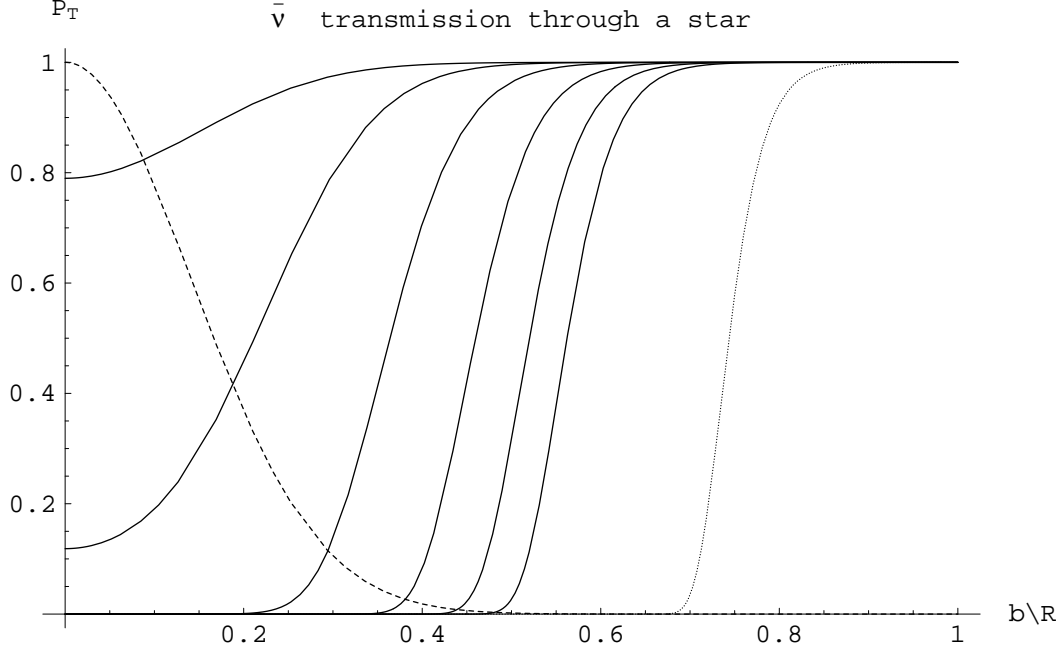


Figure 6: Transmission probability in function of b , the impact parameter, for an antineutrino energy $E_{\bar{\nu}} = 10$ GeV, 10^2 GeV, 10^3 GeV, 10^4 GeV, 10^5 GeV, 10^6 GeV (solid lines, from left to right). Dashed line on the right is for $E_{\bar{\nu}} = 6.3$ PeV and corresponds to $\bar{\nu}_e e^-$ scattering.

(of the order of $10^{19} eV$)[7] and we may neglect them in our present frame of work.

Concerning the visible part of the Galaxy, a rough estimate gives an average density of stars of $1 pc^{-3}$, which corresponds to a negligible probability for the neutrino to encounter a star during its passage through the galaxy, even in the worst case if it traverses the whole disk and the bulge.

We thus conclude that the passage of neutrinos through the galaxy won't decrease their flux, and hence do not affect the lensing effect.

4 Signal enhancement

4.1 Geometry

4.1.1 General relations

While a significant enhancement will only be reached for well - aligned lens, detector and source, we need to consider unaligned elements when dealing with extended sources or when taking into account the detector size. We follow closely [8], and remind the basic geometric relations

$$\beta = \theta - \frac{D_{LS}}{D_{SO}}\alpha \quad (38)$$

where α ⁹ is the deflection angle; β , the angular position of the source and θ , the angular position of the image. See Fig. (7).

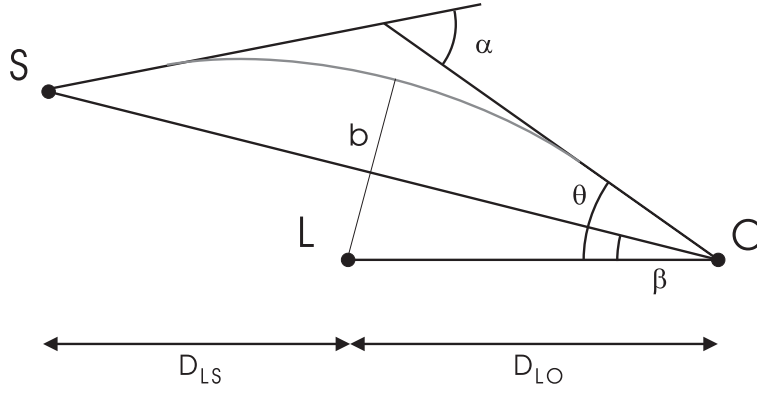


Figure 7: The geometry of the lensing event. The lens is located at a distance D_{OL} from the observer; the source, at a distance D_{SO} . The angular separation between the lens and the source is an angle β and the position of the image is at an angle θ . The deflection angle is α .

This relation is equivalent to:

$$\beta = \theta - \frac{\theta_0^2}{\theta} \quad (39)$$

$$\text{or} \quad \beta D_{LO} = b - \frac{b_0^2}{b} \quad (40)$$

⁹So far, it has been called $\Delta\phi$.

where θ_0, b_0 are the values of θ, b in the case of perfect alignment. The deflection, the characteristic length and angle obey:

$$\begin{aligned}\alpha &= \frac{4M}{b}g(b) \\ b_0 &= \theta_0 D_{LO} = \sqrt{4Mg(b) \cdot \frac{D_{LO}D_{LS}}{D_{SO}}} \\ \theta_0 &= \frac{b_0}{D_{LO}} = \sqrt{4Mg(b) \cdot \frac{D_{LS}}{D_{LO}D_{SO}}}\end{aligned}\tag{41}$$

where $2M = \frac{2GM}{c^2} = R_{Schw.}$ is the Schwartzschild radius of the lens (M is its mass).

If $R_L < b$ (R_L is the radius of the lens), we are in the usual (photon) case (OUTcase): the deflection is given by $4M/b$ and $g(b) = 1$.

As we have seen in section 2, in general $g(b) \neq 1$, and explicit expressions were given for Newtonian objects, assuming either Gaussian or Lorentzian density profiles.

An interesting quantity is the focal length f of the lens for given b :

$$f(b) = \left(\frac{4Mg(b)}{b^2} \right)^{-1}\tag{42}$$

A constant $f(b)$ would signal a perfect lens, where a plane wave focuses in one point. Solving graphically $f = D_{LO}$ determines whether lensing occurs, and what its quality is.

4.1.2 Alignment

To observe neutrino lensing will usually require huge amplification, and we will see that this only happens in the case of perfect alignment ($\beta = 0$). An interesting situation occurs when, in a region of b , say $[b_{min}, b_{max}]$,

$$g(b) = \gamma b^2\tag{43}$$

$$\sqrt{4M\gamma \cdot \frac{D_{LO}D_{LS}}{D_{SO}}} \approx 1\tag{44}$$

In this case indeed the deflection angle is proportional to b , the focal length is nearly constant and the object becomes a good lens: all the neutrinos in that region of b are focused on the same point. (The second equation simply puts the observer at the focus).

In this situation, all the particles passing through a ring $[b_{min}, b_{max}]$ or even the full disk if $b_{min} = 0$ focus on the detector. The signal enhancement is then given by the ratio of the area of this ring or disk to the area of the corresponding disk in case no lensing happens. For a Gaussian density profile, the region $[0, r_0]$ has a reasonably good lens behavior. Slightly outside of the focus area, either a ring or disk would in principle be observed, but this requires an angular resolution and statistics unrealistic for neutrinos; our only hope is to notice the enhancement factor.¹⁰

4.2 Amplification factor.

4.2.1 General relations.

The most general relation for the magnification (here, the signal enhancement) μ is [8]:

$$\mu = \frac{\Delta\Omega}{\Delta\Omega_0} = \left| \det \frac{\partial \vec{\beta}}{\partial \vec{\theta}} \right|^{-1} = \frac{\mathcal{A}}{\mathcal{A}_0} = \left| \frac{\theta_i \Delta\theta_i}{\beta \Delta\beta} \right| \quad (45)$$

where $\Delta\Omega$, $\Delta\Omega_0$ stand for the solid angle that the particle trajectories span in the sky, respectively with and without lensing effect;

$\vec{\beta}$, $\vec{\theta}$ are the angular coordinates of the source and the image;

\mathcal{A} , \mathcal{A}_0 are the surfaces of the source and the image referred in a same plane (for instance source or lens plane);

The last equality holds because $\vec{\beta}$ and $\vec{\theta}$ are aligned. The index i refers to a specific image (in general there is more than one).

The calculation of the magnification depends on the relation between β and θ (given by Eqs. (38,41)).

¹⁰It is in principle possible to obtain more than one ring, if $f(b)$ crosses $f = D_{LO}$ more than once, although this does not happen for the Gaussian and the Lorentzian density profiles.

In the OUTcase, we have two images and the resulting magnification is well known:

$$\mu_{\pm} = \frac{1}{4} \left(\frac{\beta}{\sqrt{\beta^2 + 4\theta_0^2}} + \frac{\sqrt{\beta^2 + 4\theta_0^2}}{\beta} \pm 2 \right) \quad (46)$$

$$\mu = \mu_+ + \mu_- = \frac{\beta^2 + 2\theta_0^2}{\beta\sqrt{\beta^2 + 4\theta_0^2}} \quad (47)$$

$$\mu \xrightarrow{\beta \rightarrow 0} \frac{\theta_0}{\beta} \stackrel{def}{=} \mu_{OUT}^{\beta} \quad (48)$$

For the INcase, no general relation holds but we will consider two simplified cases (linear and quadratic):

$$\text{If } g(b) = \gamma b^2, \alpha = 4M\gamma b \Rightarrow \mu_i = \left(\frac{\theta(\beta)}{\beta} \right)^2 \stackrel{def}{=} \mu_{disk}^{\beta} = \text{const.} \quad (49)$$

A Gaussian density profile, taken close to the center is similar to the quadratic case. Note the surprising result that the magnification is independent of β . As $g(b) = \gamma b^2$ only between $b = 0$ and $b = r_0$ (for the Gaussian profile), the relation holds for $\beta \leq r_0/D_{LO}$. The well known OUTcase behavior is recovered for $\beta \gg r_0/D_{LO}$.

$$\text{If } g(b) = \delta b, \alpha = 4M\delta \Rightarrow \mu_i = 1 + \frac{D_{SL}}{D_{SO}} \frac{\alpha}{\beta} = 1 + \frac{\theta_0^2}{\theta\beta} \xrightarrow{\beta \rightarrow 0} \frac{\theta_0}{\beta} \quad (50)$$

The linear case occurs near $b = r_0$ with both Gaussian and Lorentzian profiles. There is only a significant magnification near alignment. Otherwise, the lens only refracts the signal: it just changes the apparent position of the source.

4.2.2 Alignment.

Extended sources. This far, we have only considered point-like sources and detectors, and as a result, their magnification appears to diverge when

source, lens and detector are aligned Eq. (46). For an extended circular source of uniform brightness and of angular radius θ_S , the magnification factor (OUTcase) is [8]:

$$\mu_{OUT}^S = \frac{1}{\pi\theta_S^2} \int_0^{\theta_S} 2\pi\beta d\beta \mu(\beta) \quad (51)$$

$$= \frac{\sqrt{\theta_S^2 + 4\theta_0^2}}{\theta_S} \quad (52)$$

$$\xrightarrow{\theta_S \rightarrow 0} \frac{2\theta_0}{\theta_S} \quad (53)$$

For the INcase, one evaluates the integral above in the same way, using the relations (38,41). For the case $g(b) = \gamma b^2$, i.e. $\alpha = 4M\gamma b$, the image of the source (in the lens plane for instance) is a full disk of angular radius $\theta_{disk} = r_0/D_{LO}$. The amplification factor is then ¹¹

$$\mu_{disk}^S = \frac{\mathcal{A}}{\mathcal{A}_0} = \left(\frac{\theta_{disk}}{\theta_S} \right)^2 \quad (54)$$

For the case $\alpha = 4M\delta$, during alignment, the image of the source is a ring of radius θ_0 and width $\sim \theta_S$. In the limit $\theta_S \rightarrow 0$, the amplification is the same as in the OUTcase:

$$\mu^S = \frac{\mathcal{A}}{\mathcal{A}_0} = 1 + \frac{2\theta_0^2}{\theta\theta_S} \xrightarrow{\theta_S \rightarrow 0} \frac{2\theta_0}{\theta_S} \quad (55)$$

Extended detector. Finally, we discuss the case of point-like source aligned with the lens and the observer. At first glance, the magnification, μ^β or μ^S diverges. However, we have not yet taken into account the finite size of the detector. The geometry of our problem is symmetric: one can exchange β for

¹¹ When evaluating the integral, one must substitute $\int_0^{\theta_S}$ by $\int_0^{\theta_{disk}/\sqrt{\mu^\beta}}$. This takes into account the finite size of the lens: the relation $\alpha = 4M\gamma b$ holds only in the interval $[0; \theta_{disk}]$.

β_ϕ (the angle \widehat{LSO}), D_{LS} for D_{LO} and θ_S for θ_ϕ , the latter being the angular radius of the detector seen from the source. The amplification then reads:

$$\mu_{OUT}^\phi = \frac{2\theta_0}{\theta_\phi} \frac{D_{LO}}{D_{LS}} \quad (56)$$

$$\mu_{disk}^\phi = \left(\frac{\theta_{disk}}{\theta_\phi} \frac{D_{LO}}{D_{LS}} \right)^2 \quad (57)$$

The factor D_{LO}/D_{LS} is due to the fact that the angle θ_ϕ is not viewed from the observer but from the source. When we evaluate the magnification, i.e. the surface of the image with and without lensing effect, we have to refer to a same plane. Doing so leads to the factor D_{LO}/D_{LS} .

Resulting amplification. Until now we have preferred a description with angles. Maybe the situation is clearer if we translate the expressions into distances in a given reference plane

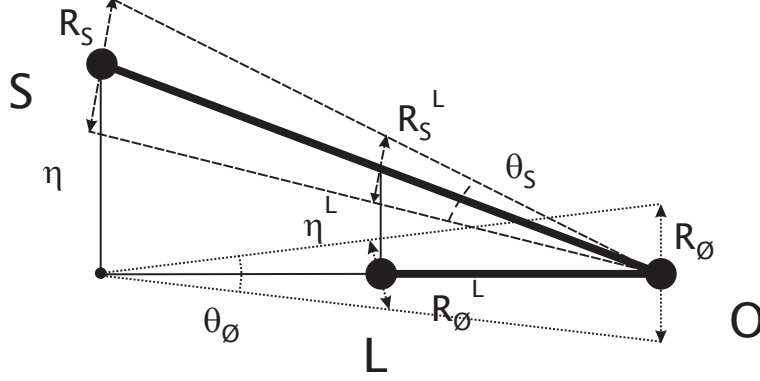


Figure 8: To the angular language corresponds formulations in distances referred to a same plane. Here, we refer in the lens plane. Ex: The source has an angular separation from the lens β , which corresponds to a distance η in the source plane or equivalently η^L in the lens plane.

Choosing to evaluate quantities in the lens plane, $\theta_0 \rightarrow \theta_0 D_{LO} = b_0$, $\theta_S \rightarrow \theta_S D_{LO} = R_S^L$, the radius of the source in the lens plane, $\beta \rightarrow \beta D_{LO} = \eta^L$, the position of the source in the lens plane, and $\theta_\phi D_{LS}/D_{LO} \rightarrow \theta_\phi D_{LS} = R_\phi^L$,

the radius of the detector in the lens plane, as seen from the source. The magnification then reads:

$$\begin{aligned} \mu_{OUT}^\beta &= \frac{b_0}{\eta^L} & \mu_{OUT}^S &= \frac{2b_0}{R_S^L} & \mu_{OUT}^\phi &= \frac{2b_0}{R_\phi^L} \\ \mu_{disk}^\beta &= \left(\frac{b_0}{\eta^L}\right)^2 & \mu_{disk}^S &= \left(\frac{b_{disk}}{R_S^L}\right)^2 & \mu_{disk}^\phi &= \left(\frac{b_{disk}}{R_\phi^L}\right)^2 \end{aligned} \quad (58)$$

As we know by Eq. (45), the magnification factor is given by the ratio $\frac{A}{A_0}$. Which formula to apply results from a competition between the three angles β , θ_S and $\theta_\phi D_{LS}/D_{LO}$, or, equivalently, between the lengths η^L , R_S^L and R_ϕ^L . Discarding immediately the off-alignment case, we must compare two situations, using the lens plane images. If R_S^L (resp. R_ϕ^L) dominates, the image in the lens plane is a ring of width R_S^L (resp. R_ϕ^L). Finally, if the image is a disk, it is independent of the source and the detector *during the lensing* but the area of the image *without lensing* is $\pi R_S^{L^2}$ (resp. $\pi R_\phi^{L^2}$). So, the answer is: check which length (η^L , R_S^L or R_ϕ^L) is largest and use the corresponding expression for the magnification factor (resp. μ^β , μ^S or μ^ϕ). Notice the magnification factor is inversely proportional to the characteristic length, or its square, so that the smallest value for the magnification factor is always selected.

Note that in all cases we have the following requirements, in order to use the approximated expressions:

$$\beta, \theta_S, \theta_\phi \ll \theta_o \quad (59)$$

$$\eta^L, R_S^L, R_\phi^L \ll b_0 \quad (60)$$

4.3 Approximations

4.3.1 The distant source: $D_{SO} \approx D_{SL} \gg D_{LO}$

If the source is far away, the expression for the impact parameter and the magnification μ^ϕ simplifies: $b_0 \simeq \sqrt{4Mg(b)D_{LO}}$, $\theta_0 \simeq \sqrt{\frac{4Mg(b)}{D_{LO}}}$, $R_\phi^L \simeq R_\phi$, $\mu_{OUT}^\phi \simeq \frac{2b_0}{R_\phi}$, $\mu_{disk}^\phi \simeq \left(\frac{b_{disk}}{R_\phi}\right)^2$. The following inequalities hold: $\eta^L \ll \eta$, $R_S^L \ll R_S$.

A consequence is that in this case one should take care for R_ϕ . Indeed, it is possible that $R_S^L \ll R_\phi$; then the magnification μ^ϕ applies.

4.3.2 Binary systems: $D_{SO} \approx D_{LO} \gg D_{LS}$

If the source and the lens are close to each other, as for binary systems¹² (one object being the lens; the other, the source¹³), the impact parameter and the magnification μ^S simplifies: $b_0 \simeq \sqrt{4Mg(b) D_{LS}}$, $\theta_0 \simeq \sqrt{\frac{4Mg(b) D_{LS}}{D_{LO}^2}}$, $R_S^L \simeq R_S$,

$\mu_{OUT}^S \simeq \frac{2b_0}{R_S}$ and $\mu_{disk}^S \simeq \left(\frac{b_{disk}}{R_S}\right)^2$. We have also: $\eta^L \simeq \eta$ and $R_\phi^L \ll R_\phi$.

As $R_\phi \leq 1$ km and as the source is usually macroscopic $R_S \gg 1$ km, it is never needed to take into account the finite size of the detector. So μ^ϕ never applies. For binary systems the most dangerous approximation is $R_S \ll b_0$. This should be checked. If this is not realized, one should use the full expressions, Eqs. (46,51).

5 Applications

We will now concentrate on possible applications and a few examples. In practice, we first test if we are in an OUTcase or not. Then we determine the expected shape of the image (discussion of the intersection of $f(b)$ with $f = D_{LO}$ and its characteristics. We estimate the magnification by determining the largest length between η^L , R_S^L and R_ϕ^L . We check all these lengths are smaller than b_0 to know if we may apply the approximations for the magnification. Finally, we compute the expected signal for a given detector (in our case Super-Kamiokande, SK, or IceCube).

5.1 The Sun

We consider the Sun as a first example.

Neutrinos passing outside the Sun don't focus close enough to Earth to be of use; in fact for them to focus on Earth, we would need

$$b_0 \simeq 30.000\text{km} \simeq 5\% R_\odot \quad (61)$$

which is clearly well inside the Sun, so the OUT solution does not provide any sizeable effect.

¹²Henceforth "binary systems" will point the case $D_{LO} \gg D_{LS}$

¹³For a treatment of binary systems, see Ref. [9]

We turn to the INcase, using as announced a Gaussian density profile as a reasonable approximation of the matter distribution. Unfortunately, the plot of the focal length never crosses the line $f = D_{LO} = 1$ a.u. The smallest value is at about 22 a.u., which means Uranians can perform wonderful neutrino lensing experiments using the Sun as lens. For them, any source would be amplified in turn as the Sun sweeps in front of it! (Jupiter cannot replace the Sun as a useful lens for us, as its mass is about $10^{-3}M_{\odot}$).

Even if we are not at the focal point, there is yet some amplification due to the improved convergence of the beam. It provides:

$$A = \left(\frac{f}{|f - D_{LO}|} \right)^2 \quad (62)$$

The effect is significant if $D_{LO} \simeq f$, say $D_{LO} \in [0.3f; 3f]$, to have a magnification higher than 2. Beyond $3f$, this last effect is negligible.

The Sun is thus not a good candidate amplifying a neutrino signal. Even if the neutrinos are seriously deflected, the deflection itself is in practice impossible to detect, as it has been done for photons, this is both due to the insufficient detection capacity and to the limited angular resolution: 1° in the best cases, compared to deflections of less than one arcminute.

5.2 Stars

It is well known that stars are good lens candidates. Indeed, the OUTcase test tells us:

$$b_0 \approx 20R_{\odot} \left(\frac{M}{M_{\odot}} \right)^{\frac{1}{2}} \left(\frac{D_{LO}}{\text{pc}} \right)^{\frac{1}{2}} \quad \text{if } D_{LO} \ll D_{LS} \quad (63)$$

$$b_0 \approx 30.000\text{km} \left(\frac{M}{M_{\odot}} \right)^{\frac{1}{2}} \left(\frac{D_{LS}}{\text{a.u.}} \right)^{\frac{1}{2}} \quad \text{if } D_{LO} \gg D_{LS} \quad (64)$$

where M is the mass of the lens and M_{\odot} , R_{\odot} are the solar mass and radius.

For distant sources, since the closest star is yet at about 1.3 pc, the OUTcase applies for lensing on stars. The phenomenology is the same as for photons. If the source is aligned, the image is a ring of radius b_0 . The magnification is given by:

$$\begin{aligned}
\mu_{OUT}^{\emptyset} &\approx 13 \times 10^6 \left(\frac{\text{km}}{R_{\emptyset}}\right) \left(\frac{M}{M_{\odot}}\right)^{\frac{1}{2}} \left(\frac{D_{LO}}{\text{pc}}\right)^{\frac{1}{2}} && \text{if } R_{\emptyset} \gg R_s^L \\
\mu_{OUT}^S &\approx 39.000 \left(\frac{R_{\odot}}{R_S}\right) \left(\frac{M}{M_{\odot}}\right)^{\frac{1}{2}} \left(\frac{100\text{pc}}{D_{LO}}\right)^{\frac{1}{2}} \left(\frac{D_{SO}}{10\text{kpc}}\right) && \text{if } R_{\emptyset} \ll R_s^L
\end{aligned} \tag{65}$$

The first line applies when the size of the detector determines the radius of the ring (this never happens if the source is a star or a galaxy); the second is typical for a star or a galaxy as source. However, the "normal" neutrino signal of a star (i.e., assumed to be similar to the thermonuclear reactions in the Sun) cannot be detected through such amplification. In the most favorable case (short D_{LO} and D_{SO} distances):

$$\begin{aligned}
N_{events} &= \left(\frac{L}{L_{\odot}}\right) \left(\frac{1\text{a.u.}}{D_{SO}}\right)^2 \mu_{OUT}^S N_{\odot} \\
&\approx 0.9 \times 10^{-11} \left(\frac{L}{L_{\odot}}\right) \left(\frac{R_{\odot}}{R_S}\right) \left(\frac{M}{M_{\odot}}\right)^{\frac{1}{2}} \left(\frac{100\text{pc}}{D_{SO}}\right) \left(\frac{1\text{pc}}{D_{LO}}\right)^{\frac{1}{2}} N_{\odot}
\end{aligned}$$

The situation could be different if for some reason stellar-size objects happened to be strong emitters of energetic neutrinos. In the case of stellar lenses, galaxies are in general too wide to be used as a neutrino sources: the magnification is trifling if the angular radius of the galaxy θ_S is larger than the angular radius of the ring θ_0 ¹⁴.

5.3 Binary Systems

We discuss now the INcase, which holds for binary systems. We will concentrate on the most promising situation, i.e. a good lens: as we have seen before, the image of the source is then a full disk. For our estimations, we have chosen a Gaussian density profile with $r_0 = 0.2R_L$, the latter giving the typical size of the disk. The magnification is thus:

$$\mu_{disk}^S = \left(\frac{\theta_{disk}}{\theta_S}\right)^2 = \left(\frac{r_0}{R_S^L}\right)^2 \tag{66}$$

$$\approx \frac{1}{25} \left(\frac{R_L}{R_S}\right)^2 \tag{67}$$

¹⁴ θ_S is typically larger than 10^{-6} for a galaxy and θ_0 is smaller than 10^{-6} for a star.

The source should thus be smaller than the lens by at least one order of magnitude.

The very question here is to know if the disk is focused on the observer. If the focal length at r_0 is too short, the disk effect will be negligible, and the effect will be dominated by an outer part of the lensing star (ring situation); if it is too long, no other part of the lensing star will be able to focus on the signal on the observer, and the magnification is given by Eq. (62). Notice here $\alpha = 4M\gamma b^2 \approx 4M(b/r_0)^2$ and $D_{LO} \approx D_{SO}$. We have the focal length:

$$\frac{f_{disk}}{D_{LO}} \approx 22 \left(\frac{R_L}{R_\odot} \right)^2 \left(\frac{M_\odot}{M} \right) \left(\frac{1 \text{ a.u.}}{D_{LS}} \right) \quad (68)$$

Clearly, the result $f_{disk}/D_{LO} \approx 1$ is achievable. This situation is really promising, providing the source is small enough compared to the lens, so that the magnification is significant. Binary stars will however seldom meet all the conditions; more exotic systems, with a compact and intense neutrino source, are needed.

5.4 Galaxies

We now turn to another class of lens candidates, namely galaxies or rather the galactic halos. If the source is also galaxy, which is an extended object, we will always be in the INcase. Indeed, from Eq. (41),

$$b_0 \leq \sqrt{4MD_{LO}} \approx 14 \text{ kpc} \left(\frac{M}{10^{12} M_\odot} \right)^{\frac{1}{2}} \left(\frac{D_{LO}}{\text{Gpc}} \right)^{\frac{1}{2}} \quad (69)$$

Now, the radius of galaxies is typically of this length but, since we will focus on the dark matter halo of the galaxy, the INcase applies in most situations.

From Fig. 2, the maximum deflection angle stays close to $4M/R_L$. More precisely, it is always less than $\pi/2 \cdot 4M/R_L$. So,

$$\alpha_{max} \leq 3 \times 10^{-6} \left(\frac{M}{10^{12} M_\odot} \right) \left(\frac{100 \text{ kpc}}{R_L} \right) \quad (70)$$

and, in order to focus on Earth,

$$D_{LO} > f_{min} = \frac{b_0}{\alpha_{max}} \approx 30 \text{Gpc} \left(\frac{b_0}{R_L} \right) \left(\frac{10^{12} M_\odot}{M} \right) \left(\frac{R_L}{100 \text{kpc}} \right) \quad (71)$$

Since the radius of the Universe is only about 5 Gpc, the neutrinos must pass rather near the center of the galaxy, often through its visible part. They survive however since the probability to meet a star is tiny. (at the difference of photons, which are absorbed by dust clouds).

For the Lorentzian density profile, the problem is that we have no precise idea of the value of r_0 , except that it is small enough to explain the velocity dispersion curves inside galaxies. Here, we discuss only the case $b_0 > r_0$. The deflection angle is then nearly constant: $\alpha \approx 4M/R_L \cdot [\pi/2 - (\pi/2 - 1)b]$. The image is a ring and the magnification is, providing $R_\phi \ll R_s^L$:

$$\mu^S \approx 2.8 \left(\frac{100 \text{kpc}}{R_s} \right) \left(\frac{M}{10^{12} M_\odot} \right)^{\frac{1}{2}} \left(\frac{10 \text{Mpc}}{D_{LO}} \right)^{\frac{1}{2}} \left(\frac{D_{SO}}{1 \text{Gpc}} \right)^{\frac{1}{2}} \left(\frac{D_{LS}}{1 \text{Gpc}} \right)^{\frac{1}{2}}$$

The magnification and the number of events are too tiny to be observed. As in the previous section, a small, intense neutrino source is preferable.

6 Conclusions

We have studied in some detail the lensing of neutrinos through models of astrophysical objects. The main difference with photons rests in the possibility for medium-energy neutrinos to cross even the core of stars, and this has the important result that the quality of the lens is greatly improved. This would have been very promising if the focal length of the center of the Sun happened to coincide with the radius of the Earth orbit, unfortunately this is far to be the case, and the focusing occurs closer to Uranus. Provided small and energetic sources exist, binary systems, where one of the companions is the emitter and the other a larger star, or galaxies could provide sizable enhancements of the signal.

7 Acknowledgments

This work was supported by I. I. S. N. Belgium and by the Communauté Française de Belgique (Direction de la Recherche Scientifique programme ARC).

D. Monderen and V. Van Elewyck benefit from a F. R. I. A. grant.

Appendix

In this appendix, we present the procedure for calculating the deflection of neutrinos from straight-line motion as they pass through a gravitational field produced by a compact object of mass M . Here, we only consider in detail the case concerning the INside solution, i.e. when the neutrino flux passes through the object. The procedure is shown for the three specific density profiles explained in Sec. 2: constant density, Gaussian and Lorentzian distribution densities.

The procedure starts with the calculation of the mass and pressure of the object at a radius r , $m(r)$ and $p(r)$ respectively, for a given density profile $\rho(r)$. We also calculate $\Phi(r)$ and the metric as explained in the main text. Second, we derive from the metric the equation of the orbit (for the case of constant density we show in detail the derivation) and the smallest radius reached by the particle. Finally, we calculate the net deflection.

We begin by calculating the net deflection for the case of a constant density profile $\rho(r) = \rho$

$$\begin{aligned}
 \implies m(r) &= \frac{4\pi}{3}\rho r^3 = M \left(\frac{r}{R}\right)^3 \\
 \implies p(r) &= \rho \frac{\sqrt{1 - \frac{2M}{R} \frac{r^2}{R^2}} - \sqrt{1 - \frac{2M}{R}}}{3\sqrt{1 - \frac{2M}{R}} - \sqrt{1 - \frac{2M}{R} \frac{r^2}{R^2}}} \\
 \implies e^{2\Phi(r)} &= \left(\frac{3}{2}\sqrt{1 - \frac{2M}{R}} - \frac{1}{2}\sqrt{1 - \frac{2M}{R} \frac{r^2}{R^2}} \right)^2 \\
 \implies ds^2 &= - \left(\frac{3}{2}\sqrt{1 - \frac{2M}{R}} - \frac{1}{2}\sqrt{1 - \frac{2M}{R} \frac{r^2}{R^2}} \right)^2 dt^2 + \frac{1}{1 - \frac{2M}{r} \left(\frac{r}{R}\right)^3} dr^2 + r^2 d\Omega^2 .
 \end{aligned} \tag{72}$$

For a massless particle

$$\left. \begin{aligned} p_0 &= -E \\ p^r &= \frac{dr}{d\lambda} \\ p_\phi &= L \end{aligned} \right\} \Rightarrow \left\{ \begin{aligned} p^0 &= \frac{E}{\left(\frac{3}{2} \sqrt{1 - \frac{2M}{R}} - \frac{1}{2} \sqrt{1 - \frac{2M}{R} \frac{r^2}{R^2}} \right)^2} \\ p_r &= \frac{1}{1 - \frac{2M}{r} \left(\frac{r}{R} \right)^3} \frac{dr}{d\lambda} \\ p^\phi &= \frac{d\phi}{d\lambda} = \frac{L}{r^2} \end{aligned} \right. \quad (73)$$

and the equation of the orbit ($p^2 = 0$) is then

$$\begin{aligned} \frac{d\phi}{dr} &= \frac{\frac{3}{2} \sqrt{1 - \frac{2M}{R}} - \frac{1}{2} \sqrt{1 - \frac{2M}{R} \frac{r^2}{R^2}}}{\sqrt{1 - \frac{2M}{r} \left(\frac{r}{R} \right)^3}} \frac{1}{r^2 \sqrt{\frac{1}{b^2} - \frac{1}{r^2} \left(\frac{3}{2} \sqrt{1 - \frac{2M}{R}} - \frac{1}{2} \sqrt{1 - \frac{2M}{R} \frac{r^2}{R^2}} \right)^2}} \\ \Rightarrow \frac{d\phi}{du} &= \frac{\left(1 - \frac{3M}{2R}\right) + \frac{3M}{2R^3} \frac{1}{u^2}}{\sqrt{\left(\frac{1}{b^2} - \frac{M}{R^3}\right) - u^2 \left(1 - \frac{3M}{R}\right)}} + O(M^2 u^2) . \end{aligned} \quad (74)$$

Integrating Eq. (74) gives

$$\begin{aligned} \phi_{\text{IN}}(u) &= \phi_0 + \frac{2M}{b} \left(1 - \sqrt{1 - \frac{b^2}{R^2}} \right) + \arcsin \left[\frac{b}{R} \left(1 - \frac{M}{R} \right) \right] \\ &+ \frac{3M}{2R} \frac{b^2}{R^2} \left(\sqrt{1 - \frac{b^2}{R^2}} \frac{R}{b} - \sqrt{1 - b^2 u^2} \frac{1}{bu} \right) \\ &- \arcsin \left\{ \frac{b}{R} \left[1 - \frac{3M}{2R} \left(1 - \frac{b^2}{3R^2} \right) \right] \right\} \\ &+ \arcsin \left\{ bu \left[1 - \frac{3M}{2R} \left(1 - \frac{b^2}{3R^2} \right) \right] \right\} , \end{aligned} \quad (75)$$

where the integration constant is defined so as $\phi_{\text{IN}}(r = R) = \phi_{\text{OUT}}(r = R)$ (with ϕ_0 the initial incoming direction). The particle reaches its smallest r when $\frac{dr}{d\lambda} = 0$:

$$\begin{aligned} \frac{dr}{d\lambda} &= E \sqrt{\left[\frac{1}{\left(\frac{3}{2} \sqrt{1 - \frac{2M}{R}} - \frac{1}{2} \sqrt{1 - \frac{2M}{R} \frac{r^2}{R^2}} \right)^2} - \frac{b^2}{r^2} \right] \left[1 - \frac{2M}{r} \left(\frac{r}{R} \right)^3 \right]} = 0 \\ \Rightarrow u_{\text{max}} &= \frac{1}{b} \left[1 + \frac{3M}{2R} \left(1 - \frac{b^2}{3R^2} \right) \right] + O(M^2 u^2) , \end{aligned} \quad (76)$$

then

$$\begin{aligned} \phi_{\text{IN}}(u = u_{\text{max}}) &= \phi_0 + \frac{\pi}{2} + \frac{2M}{b} \left(1 - \sqrt{1 - \frac{b^2}{R^2}} \right) + \arcsin \left[\frac{b}{R} \left(1 - \frac{M}{R} \right) \right] \\ &+ \frac{3M}{2R} \frac{b}{R} \sqrt{1 - \frac{b^2}{R^2}} - \arcsin \left\{ \frac{b}{R} \left[1 - \frac{3M}{2R} \left(1 - \frac{b^2}{3R^2} \right) \right] \right\} , \end{aligned} \quad (77)$$

and the net deflection is

$$\begin{aligned}
\Delta\phi &= \begin{cases} \frac{4M}{b} & \text{if } b \geq R \\ \frac{4M}{b} \left(1 - \sqrt{1 - \frac{b^2}{R^2}}\right) + 2 \arcsin \left[\frac{b}{R} \left(1 - \frac{M}{R}\right)\right] \\ \quad + \frac{3M}{R} \frac{b}{R} \sqrt{1 - \frac{b^2}{R^2}} - 2 \arcsin \left\{\frac{b}{R} \left[1 - \frac{3M}{2R} \left(1 - \frac{b^2}{3R^2}\right)\right]\right\} & \text{if } b < R \end{cases} \\
&= \begin{cases} \frac{4M}{b} & \text{if } b > R \\ \frac{4M}{R} & \text{if } b = R \\ \frac{4M}{R} \frac{3b}{2R} & \text{if } b \ll R \\ 0 & \text{if } b = 0 \end{cases}
\end{aligned} \tag{78}$$

where the outside solution is also included for completeness.

Next, we present the analysis for the Gaussian and Lorentzian distribution densities. As explained in the main text, in both cases, it is possible to make some approximations (see Eqs. (15,16) in Sec. 2) that allow us to derive an analytical expression for the net deflection. For a Gaussian distribution density profile $\rho(r) = \rho_0 e^{-r^2/r_0^2}$

$$\begin{aligned}
\Rightarrow m(r) &= M \frac{r}{R} e^{(R^2 - r^2)/r_0^2} \frac{r_0/r e^{r^2/r_0^2} \sqrt{\pi}/2 \operatorname{erf}(r/r_0) - 1}{r_0/R e^{R^2/r_0^2} \sqrt{\pi}/2 \operatorname{erf}(R/r_0) - 1} \\
\Rightarrow \Phi(r) &= -\frac{M}{R} \frac{r_0/r e^{R^2/r_0^2} \sqrt{\pi}/2 \operatorname{erf}(r/r_0) - 1}{r_0/R e^{R^2/r_0^2} \sqrt{\pi}/2 \operatorname{erf}(R/r_0) - 1} \\
\Rightarrow ds^2 &= -\left(1 - \frac{2M}{R} \frac{r_0/r e^{R^2/r_0^2} \sqrt{\pi}/2 \operatorname{erf}(r/r_0) - 1}{r_0/R e^{R^2/r_0^2} \sqrt{\pi}/2 \operatorname{erf}(R/r_0) - 1}\right) dt^2 \\
&\quad + \left(1 + \frac{2M}{R} e^{(R^2 - r^2)/r_0^2} \frac{r_0/r e^{r^2/r_0^2} \sqrt{\pi}/2 \operatorname{erf}(r/r_0) - 1}{r_0/R e^{R^2/r_0^2} \sqrt{\pi}/2 \operatorname{erf}(R/r_0) - 1}\right) dr^2 + r^2 d\Omega^2,
\end{aligned} \tag{79}$$

where the error function is defined as $\operatorname{erf}(z) = \frac{2}{\sqrt{\pi}} \int_0^z dt e^{-t^2}$. The equation of

the orbit is

$$\begin{aligned} \frac{d\phi}{dr} &= \left[1 - \frac{M}{R} \frac{e^{(R^2-r^2)/r_0^2}-1}{r_0/R e^{R^2/r_0^2} \sqrt{\pi}/2 \operatorname{erf}(R/r_0)-1} \right] \frac{1}{r^2 \sqrt{\frac{1}{b^2} - \frac{1}{r^2} \left[1 - \frac{2M}{R} \frac{r_0/r e^{R^2/r_0^2} \sqrt{\pi}/2 \operatorname{erf}(r/r_0)-1}{r_0/R e^{R^2/r_0^2} \sqrt{\pi}/2 \operatorname{erf}(R/r_0)-1} \right]}} \\ \Rightarrow \frac{d\phi}{dy} &= \left\{ 1 + \frac{2M}{R} \frac{e^{R^2/r_0^2} [\sqrt{\pi}/2 y r_0 \operatorname{erf}(1/y r_0) - e^{-1/(y r_0)^2}]}{r_0/R e^{R^2/r_0^2} \sqrt{\pi}/2 \operatorname{erf}(R/r_0)-1} \right\} \frac{1}{\sqrt{\frac{1}{b^2} - y^2}} + O(M^2 u^2), \end{aligned} \quad (80)$$

where y is defined as

$$y \equiv \frac{1}{r} \left[1 - \frac{M}{R} \frac{r_0/r e^{R^2/r_0^2} \sqrt{\pi}/2 \operatorname{erf}(r/r_0) - 1}{r_0/R e^{R^2/r_0^2} \sqrt{\pi}/2 \operatorname{erf}(R/r_0) - 1} \right]. \quad (81)$$

Integrating Eq. (80) gives

$$\begin{aligned} \phi_{\text{IN}}(y) &= \phi_0 + \frac{2M}{b} \left(1 - \sqrt{1 - \frac{b^2}{R^2}} \right) + \arcsin(by) \\ &+ \frac{2M}{b} \frac{r_0/R e^{R^2/r_0^2} \sqrt{\pi}/2}{r_0/R e^{R^2/r_0^2} \sqrt{\pi}/2 \operatorname{erf}(R/r_0)-1} \\ &\times \left\{ \sqrt{1 - \frac{b^2}{R^2}} \operatorname{erf}(R/r_0) - \sqrt{1 - b^2 y^2} \operatorname{erf}(1/y r_0) \right. \\ &\quad \left. - e^{-b^2/r_0^2} \left[\operatorname{erf} \left(\sqrt{1 - \frac{b^2}{R^2}} \frac{R}{r_0} \right) - \operatorname{erf} \left(\frac{\sqrt{1 - b^2 y^2}}{y r_0} \right) \right] \right\}. \end{aligned} \quad (82)$$

The particle reaches its smallest r at $y_{\text{max}} = \frac{1}{b} + O(M^2 u^2)$, then

$$\begin{aligned} \phi(y = \frac{1}{b}) &= \phi_0 + \frac{\pi}{2} + \frac{2M}{b} \left(1 - \sqrt{1 - \frac{b^2}{R^2}} \right) + \frac{2M}{b} \frac{r_0/R e^{R^2/r_0^2} \sqrt{\pi}/2}{r_0/R e^{R^2/r_0^2} \sqrt{\pi}/2 \operatorname{erf}(R/r_0)-1} \\ &\times \left[\sqrt{1 - \frac{b^2}{R^2}} \operatorname{erf}(R/r_0) - e^{-b^2/r_0^2} \operatorname{erf} \left(\sqrt{1 - \frac{b^2}{R^2}} \frac{R}{r_0} \right) \right], \end{aligned} \quad (83)$$

and the net deflection is

$$\begin{aligned}
\Delta\phi &= \begin{cases} \frac{4M}{b} & \text{if } b \geq R \\ \frac{4M}{b} \left(1 - \sqrt{1 - \frac{b^2}{R^2}}\right) + \frac{4M}{b} \frac{r_0/R e^{R^2/r_0^2} \sqrt{\pi}/2}{r_0/R e^{R^2/r_0^2} \sqrt{\pi}/2 \operatorname{erf}(R/r_0) - 1} \\ \quad \times \left\{ \sqrt{1 - \frac{b^2}{R^2}} \operatorname{erf}(R/r_0) - e^{-b^2/r_0^2} \operatorname{erf}\left(\sqrt{1 - \frac{b^2}{R^2}} \frac{R}{r_0}\right) \right\} & \text{if } b < R \end{cases} \\
&= \begin{cases} \frac{4M}{b} & \text{if } b > R \\ \frac{4M}{R} & \text{if } b = R \\ \frac{4M}{R} \frac{e^{R^2/r_0^2} \sqrt{\pi}/2 \operatorname{erf}(R/r_0)}{r_0/R e^{R^2/r_0^2} \sqrt{\pi}/2 \operatorname{erf}(R/r_0) - 1} \frac{b}{r_0} & \text{if } b \ll R \\ 0 & \text{if } b = 0 \end{cases}
\end{aligned} \tag{84}$$

For a Lorentzian distribution density profile $\rho(r) = \frac{\rho_0}{1+r^2/r_0^2}$

$$\begin{aligned}
\Rightarrow m(r) &= M \frac{r}{R} \frac{1-r_0/r \arctan(r/r_0)}{1-r_0/R \arctan(R/r_0)} \\
\Rightarrow \Phi(r) &= -\frac{M}{R} \frac{1-r_0/r \arctan(r/r_0) - \frac{1}{2} \log\left(\frac{r^2+r_0^2}{R^2+r_0^2}\right)}{1-r_0/R \arctan(R/r_0)} \\
\Rightarrow ds^2 &= -\left(1 - \frac{2M}{R} \frac{1-r_0/r \arctan(r/r_0) - \frac{1}{2} \log\left(\frac{r^2+r_0^2}{R^2+r_0^2}\right)}{1-r_0/R \arctan(R/r_0)}\right) dt^2 \\
&\quad + \left(1 + \frac{2M}{R} \frac{1-r_0/r \arctan(r/r_0)}{1-r_0/R \arctan(R/r_0)}\right) dr^2 + r^2 d\Omega^2 .
\end{aligned} \tag{85}$$

The equation of the orbit is

$$\begin{aligned}
\frac{d\phi}{dr} &= \left[1 + \frac{M}{R} \frac{\frac{1}{2} \log\left(\frac{r^2+r_0^2}{R^2+r_0^2}\right)}{1-r_0/R \arctan(R/r_0)}\right] \frac{1}{r^2 \sqrt{\frac{1}{b^2} - \frac{1}{r^2} \left[1 - \frac{2M}{R} \frac{1-r_0/r \arctan(r/r_0) - \frac{1}{2} \log\left(\frac{r^2+r_0^2}{R^2+r_0^2}\right)}{1-r_0/R \arctan(R/r_0)}\right]}} \\
\Rightarrow \frac{d\phi}{dy} &= \left[1 + \frac{2M}{R} \frac{1-r_0 y \arctan(1/r_0 y)}{1-r_0/R \arctan(R/r_0)}\right] \frac{1}{\sqrt{\frac{1}{b^2} - y^2}} + O(M^2 u^2) ,
\end{aligned} \tag{86}$$

where y is defined as

$$y \equiv \frac{1}{r} \left[1 - \frac{M}{R} \frac{1 - r_0/r \arctan(r/r_0) - \frac{1}{2} \log \left(\frac{r^2 + r_0^2}{R^2 + r_0^2} \right)}{1 - r_0/R \arctan(R/r_0)} \right]. \quad (87)$$

Integrating Eq. (86) gives

$$\begin{aligned} \phi_{\text{IN}}(y) = & \phi_0 + \frac{2M}{b} \left(1 - \sqrt{1 - \frac{b^2}{R^2}} \right) + \arcsin(by) - \frac{2M}{b} \frac{1}{1 - r_0/R \arctan(R/r_0)} \frac{r_0}{R} \\ & \times \left\{ \sqrt{1 - \frac{b^2}{R^2}} \arctan(R/r_0) - \sqrt{1 - b^2 y^2} \arctan(1/r_0 y) \right. \\ & \left. - \sqrt{1 + \frac{b^2}{r_0^2}} \left[\arctan \left(\frac{\sqrt{1 - \frac{b^2}{R^2}} R}{\sqrt{1 + \frac{b^2}{r_0^2}} r_0} \right) - \arctan \left(\frac{\sqrt{1 - b^2 y^2}}{\sqrt{1 + \frac{b^2}{r_0^2}}} \frac{1}{r_0 y} \right) \right] \right\}. \end{aligned} \quad (88)$$

The particle reaches its smallest r at $y_{\text{max}} = \frac{1}{b} + O(M^2 u^2)$, then

$$\begin{aligned} \phi(y = \frac{1}{b}) = & \phi_0 + \frac{\pi}{2} + \frac{2M}{b} \left(1 - \sqrt{1 - \frac{b^2}{R^2}} \right) - \frac{2M}{b} \frac{1}{1 - r_0/R \arctan(R/r_0)} \frac{r_0}{R} \\ & \times \left[\sqrt{1 - \frac{b^2}{R^2}} \arctan(R/r_0) - \sqrt{1 + \frac{b^2}{r_0^2}} \arctan \left(\frac{\sqrt{1 - \frac{b^2}{R^2}} R}{\sqrt{1 + \frac{b^2}{r_0^2}}} \frac{1}{r_0} \right) \right], \end{aligned} \quad (89)$$

and the net deflection is

$$\begin{aligned} \Delta\phi = & \begin{cases} \frac{4M}{b} & \text{if } b \geq R \\ \frac{4M}{b} \left(1 - \sqrt{1 - \frac{b^2}{R^2}} \right) - \frac{4M}{b} \frac{1}{1 - r_0/R \arctan(R/r_0)} \frac{r_0}{R} \\ & \times \left[\sqrt{1 - \frac{b^2}{R^2}} \arctan(R/r_0) - \sqrt{1 + \frac{b^2}{r_0^2}} \arctan \left(\frac{\sqrt{1 - \frac{b^2}{R^2}} R}{\sqrt{1 + \frac{b^2}{r_0^2}}} \frac{1}{r_0} \right) \right] & \text{if } b < R \end{cases} \\ = & \begin{cases} \frac{4M}{b} & \text{if } b > R \\ \frac{4M}{R} & \text{if } b = R \\ \frac{2M}{R} \frac{\arctan(R/r_0)}{1 - r_0/R \arctan(R/r_0)} \frac{b}{r_0} & \text{if } b \ll R \\ 0 & \text{if } b = 0 \end{cases} \end{aligned} \quad (90)$$

References

- [1] B. F. Schutz, *A first course in general relativity*, Cambridge University Press 1985.
- [2] R. Gandhi *et al.*, Phys. Rev. **D58**, 093009 (1998).
- [3] CDHS Collab., H. Abramowicz *et al.*, Z. Phys. **C25** (1984), 29.
- [4] WA25 Collab., D. Allasia *et al.*, Nucl. Phys. **B307** (1981), 1.
- [5] R. Gandhi *et al.*, Astropart. Phys. **5** (1996), 81.
- [6] G. Ingelman and M. Thunman, Phys. Rev. **D54** (1996), 4385.
- [7] E. Roulet, Phys. Rev. **D47**, 12 (1993), 5247.
- [8] P. Schneider, J. Ehlers and E. E. Falco, *Gravitational Lenses*, A&A Library, Springer Verlag 1992.
- [9] E. Roulet and S. Mollerach, Phys. Rept. 279 (1997), 67.